Magnetic Grid Complexes

DOI: 10.1002/anie.200701840

A Self-Assembled, Magnetically Coupled Square Cu_{16} $4 \times [2 \times 2]$ Grid**

*Louise N. Dawe and Laurence K. Thompson**

Self-assembly strategies in coordination chemistry have reached a level of maturity such that predictable structures can be created by the simple expedient of designing and synthesizing a ligand with suitably encoded coordination information. With an appropriate balance between the coordinating features of the ligand and the coordination requirements of a metal, square $[n \times n]$ grid structures have been achieved routinely for $n = 2$ and 3 (M_4, M_9) with six-coordinate transition-metal ions (M_4: M = Mn^{II}, Co^{II}, Ni^{II}, Cu^{II}, Zn^{II}; M_9: M = Mn^{II}, Fe^{III}, Cu^{II}, Zn^{II}), using ditopic and tritopic (Scheme 1) picolylhydrazone ligands, respectively.

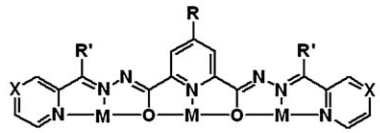

2poap (R=H, R'=NH_2, X=CH),Cl2poap (R=Cl, R'=NH_2, X=CH), 2popp (R=H, R'=Ph, X=CH), Cl2popp (R=Cl, R'=Ph, X=CH), Cl2poapz (R=Cl, R'=NH_2, X=N)

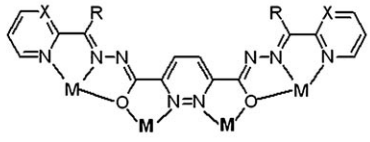

L1 (R=NH_2, X=CH), L2 (R=H, X=CH), L3(R=NH_2, X=N)

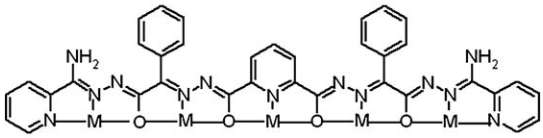

L4

Scheme 1. Tritopic, tetratopic, and pentatopic ligands.

Spin-exchange interactions occur between the paramagnetic metal ions through direct bridging (e.g. μ-O, μ-NN) connections.[1–3] The ability to concentrate spin-bearing sites in ordered "flat" arrays has created a broad interest in such systems within the chemistry and physics communities;[4–7] this interest has focused on their novel quantum-based magnetic properties, and in particular, in the case of $[Mn^{II}_5Mn^{III}_4]$ mixed-spin-state $[3 \times 3]$ grids, their potential to act as spin "qubits".[7]

The coordination capacity of such ligands can be expanded to "tetratopic" by starting with a central dinucleating pyridazine fragment, rather than pyridine (Scheme 1), and using similar extension strategies. The tetratopic pyridazine bishydrazone ligand L1 was shown to produce a linear trinuclear Ni^{II} complex,[8] with an empty potential coordination site (occupied by water), and a open, square-based, incomplete Cu_{12} $[n \times n]$ grid.[9] Other pyridazine-based polytopic ligands include tritopic and pentatopic examples, which produce a $[3 \times 3]$ Ag_9 grid complex[10] and a $2 \times [2 \times 5]$ Ag_{20} incomplete gridlike complex, respectively,[11] in which the pyridazine groups act as bridges, and the congruence of the bidentate ligand pockets creates four-coordinate (N_4) metal sites. A recent review article highlights a number of $[n \times n]$ grid-based systems in this general class.[12]

The Schiff base ligand L2 was recently shown to produce the expected $[4 \times 4]$ M_{16} grid with Mn^{II}.[13] A mixture of μ-O (hydrazone and OH) and pyridazine bridges in this compact grid arrangement of $S = 5/2$ spin centers led to intramolecular antiferromagnetic exchange. This ligand type has now been modified further to introduce pyrimidine end groups (e.g. L3). Pentatopic 2,6-bis(picolyl)hydrazone ligands have also been prepared by first creating an extended ester, converting it into the corresponding extended bishydrazone, and then capping with a pyridine function (e.g. L4). The anticipated $[5 \times 5]$ grid has been produced with Mn^{II}[14] and displays unusual magnetic properties, which are dominated by intramolecular antiferromagnetic exchange with a large residual ground-state spin.

Reaction of L3 with $Cu(CF_3SO_3)_2$ in $MeOH/CH_3CN$ led to the formation of a brown solution, from which brown crystals of $[(L3)_8Cu_{16}(O)_2(OH)_4(H_2O)_2](CF_3SO_3)_6(H_2O)_{66}(CH_3OH)_{10}$ (**1**) were obtained. The crystal structure revealed a square grid arrangement of 16 six-coordinate Cu^{II} ions embedded in an assembly of eight ligands, arranged in two roughly parallel groups of four, above and below the metal pseudoplane (Figure 1). The overall molecular dimensions for **1** involve a square cation approximately 19×19 Å^2 with a metallic core 10.9×11.2 Å^2.

A simplified core structure is shown in Figure 2. The overall structure is best considered as a combination of four square Cu_4-$(\mu\text{-}O_{hydrazone})_4$ subunits, with each subunit bridged to its neighbors by a combined $\mu\text{-}NN_{pyridazine}/\mu\text{-}O$ double bridge, in which the oxygen is exogenous. The overall

[*] L. N. Dawe, Prof. Dr. L. K. Thompson
Department of Chemistry
Memorial University
St. John's NL A1B 3X7 (Canada)
Fax: (+1) 709-737-3702
E-mail: lthomp@mun.ca

[**] This study was supported by the Natural Sciences and Engineering Research Council of Canada (NSERC).

Supporting information for this article is available on the WWW under http://www.angewandte.org or from the author.

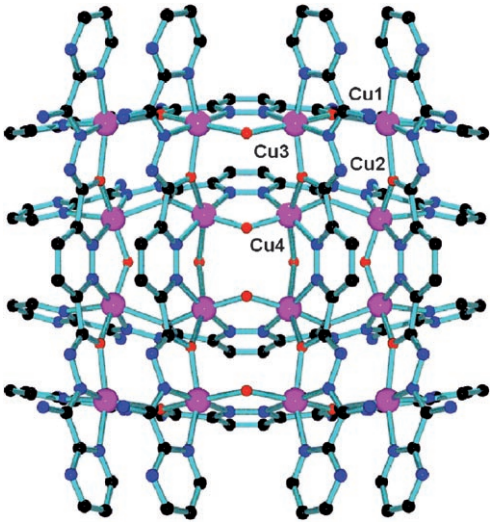

Figure 1. Povray structure of the cation in **1** (Cu magenta, N blue, O red, C black).

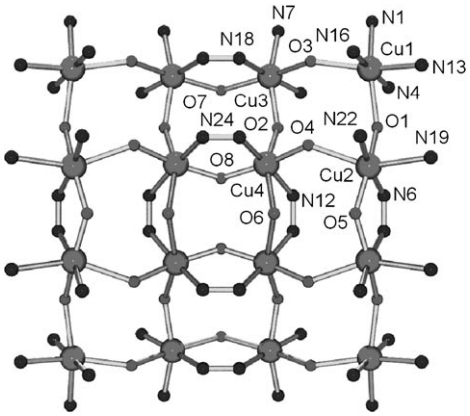

Figure 2. Povray core structure of **1**.

molecular symmetry (space group P_{mmn}) leads to four identical Cu_4 subunits related by internal mirror-plane symmetry. Cu···Cu distances within each μ-O-bridged square fall in the range 3.92–4.12 Å, and Cu-O-Cu angles are in the range 131–141°. Cu···Cu distances between the pyridazine-bridged Cu_4 subunits are smaller (3.35–3.73 Å), and as a consequence the Cu-O-Cu bridge angles are smaller (96.8–123.6°). The presence of six well-defined lattice CF_3SO_3 anions suggests nominally that 26 negative charges exist within the grid. Each ligand can reasonably be assigned a −2 charge on the basis of the normal loss of protons from the hydrazone oxygen atoms. The 10 additional negative charges are therefore reasonably associated with the exogenous oxygen bridging sites, and perhaps the ligands. The formation of hydroxide as a bridge in reactions of pyridazine-based ligands with copper(II) salts is common, even without the addition of base.[15,16] However, base was added during the synthesis of **1**, which would reasonably lead to the formation of hydroxide and even oxide. Single protons were revealed in difference maps on O5 and O6, indicating that these sites and their symmetry-related counterparts are bridging hydroxides, and two protons were found on O7, indicating a bridging water molecule at this site and its symmetry-related counterpart. No protons were found on O8, and combined with the very short Cu4–O8 bond length (1.925 Å), this strongly suggests that O8 and its symmetry-related counterpart are oxide. Other oxygen bridging sites (O1–O4) within the Cu_4 corner subunits are associated with deprotonated hydrazone oxygen atoms. This combination would lead to a total internal charge of −8 on the basis of the molecular symmetry. The two additional charges could reasonably be associated with lattice components, for example, hydroxide, but close examination of the ligand NH_2 protons revealed that H23 bound to N21 is at significantly lower occupancy than the others. Consequently, it was set to an occupancy of 0.5 in the final refinement to correctly reflect the overall charge difference, thus indicating further ligand deprotonation under basic conditions.

Each ligand (see Scheme 1) would of necessity create a bend in the arrangement of its four bound metal ions, which would be repeated throughout the grid to lead to a pronounced overall bending of the core $\{Cu_{16}(\mu\text{-}O)_{24}\}$ structure itself (Figure 3). The packing of the ligands in close

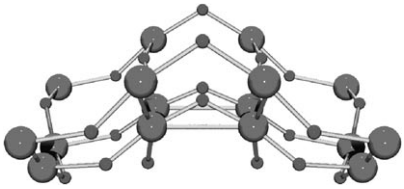

Figure 3. Core structure of **1** showing the bending (Cu large spheres, O small spheres).

proximity in roughly parallel and eclipsed pairs must add significant stability to the structure through π–π interactions and influence the choice of the preferred *syn* ligand conformation. Closest contacts between atoms in the pyridazine rings fall in the range 3.39–3.62 Å, whereas within the Cu_4 corner subunits similar pyrimidine contacts fall in the range 3.40–3.91 Å. No significant intergrid contacts were found in the extended lattice structure.

The complexity of the intragrid bridging connections would suggest that many, and perhaps all, of the bridges would contribute to the overall magnetic spin-exchange situation between the copper centers. Previous studies on simpler, and directly related, Cu_4 [2 × 2] square grids with ditopic picolinic hydrazone ligands show that Jahn–Teller distortions occur at the copper(II) sites, leading to canted (90°) orientations of the copper magnetic planes and resulting in magnetic orbital orthogonality within the grid.[1,17] The mirror-plane symmetry in **1** allows a relatively simple assessment of the magnetic-orbital connectivity by effectively considering just one quarter of the grid (Figure 4). Each corner Cu_4 subunit comprises four six-coordinate Cu^{II} ions with $\mu\text{-}O_{hydrazone}$ bridges between adjacent metal centers. Examination of Cu–L bond lengths reveals the expected Jahn–Teller elongation for Cu2, Cu3, and Cu4 (arrows in Figure 4; Cu2–O4 2.323 Å, Cu2–N19 2.468 Å, Cu3–O7

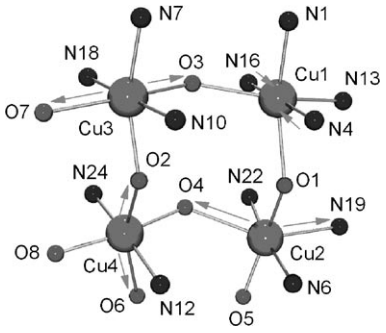

Figure 4. Jahn–Teller axes within the Cu_4-(μ-O)$_4$ corner subunits.

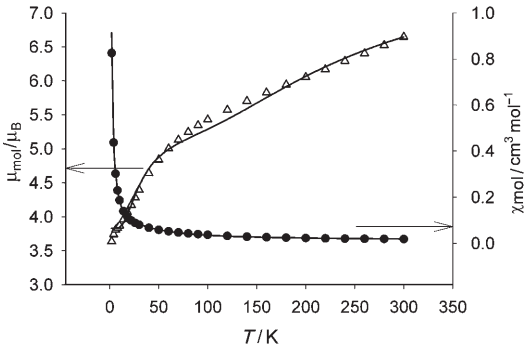

Figure 5. Plots of susceptibility and moment per mole as a function of temperature for **1** (see text for fitted parameters).

2.251 Å, Cu3–O3 2.134 Å, Cu4–O6 2.453 Å, Cu4–O2 2.193 Å), indicating $d_{x^2-y^2}$ magnetic ground states, and orthogonal connections through the oxygen bridges. This geometry would therefore suggest no antiferromagnetic exchange between Cu4 and both Cu2 and Cu3. Similar connections throughout the Cu_4 squares lead to intramolecular ferromagnetic exchange.[1,17] Cu1 is different; it has an axially compressed d_{z^2} ground state (Cu1–N4 1.932 Å, Cu1–N16 1.920 Å), which, despite the long Cu1–$O1_{hydrazone}$ bond (2.251 Å), could lead to very weak antiferromagnetic exchange between Cu1 and Cu2. The short Cu2–O5 and Cu2–$N6_{pyridazine}$ contacts (1.947 and 2.003 Å, respectively), and their symmetry-related counterparts, lead to a combination of nonorthogonal pyridazine and oxygen atom bridges. As a result, antiferromagnetic coupling would be expected for both bridging connections. Cu3 is bridged to its symmetry-related counterparts by an orthogonal oxygen bridge (O7), and a nonorthogonal pyridazine bridge, thus leading to antiferromagnetic exchange only through pyridazine. For the Cu4 centers and their symmetry-related counterparts, two bridging connections occur, through O6 and O8, leading to different bridging combinations. The oxygen O6 bridge is orthogonal, whereas oxygen O8 is nonorthogonal, but in both cases the pyridazine bridges are nonorthogonal. In those cases in which both bridges involve nonorthogonal connections it is reasonable to assume that any exchange would be considerably larger than in those cases in which just the pyridazine bridge is magnetically active.

Variable-temperature magnetic data were collected on **1** (2–300 K in a 0.1-T field). Plots of molar magnetic moment and susceptibility are shown in Figure 5. No discernible maximum was observed in the $\chi(T)$ profile, but the drop in moment on lowering the temperature clearly indicates dominant intramolecular antiferromagnetic exchange. The apparent change in slope of the $\mu(T)$ plot suggests that $|J|$ values of quite different magnitude are involved, in keeping with complex and different bridging connectivity. The room-temperature moment (6.6 μ_B) is consistent with a system comprising 16 spin-coupled Cu^{II} ions (1.65 μ_B per metal), and the moment appears to approach a slight minimum of 3.7 μ_B around 10 K, before dropping slightly below this temperature. The nonzero low-temperature moment indicates the presence of significant residual spin, which approximates the presence of four isolated Cu^{II} sites ($\mu_{calcd} = 3.8\,\mu_B$ for $g = 2.2$). The corner square Cu_4 subunits have three orthogonal internal connections, with the possibility of very weak antiferromagnetic coupling between Cu1 and Cu2. However, on the assumption that the spin-exchange connections from Cu2, Cu3, and Cu4 to other adjacent subunits are dominated by much stronger antiferromagnetic exchange (see above), the corner Cu1 sites can be considered to be essentially isolated, thus accounting for the four effective residual spins at low temperature. Magnetization data were obtained at 2 K in the range 0–5 T (Figure S1 in the Supporting Information) and show a rise in M to a value of 4.4 $N\beta$ at 5 T ($1\,N\beta = 5585\ cm^3\,Gmol^{-1}$; $M = 1.05\,N\beta$ for an integer spin at 5 T with $g = 2.21$), with no evidence for saturation. The profile is not consistent with a ground-state system with $S = 4/2$, but corresponds very closely to the sum of four independent $S = 1/2$ centers (solid line in Figure S1 calculated for $g = 2.21$ at 2 K; see below). There is no structural evidence to suggest longer range intermolecular exchange interactions.

The magnetic consequences of the bridging connections between the Cu_4 subunits would be the sum of the relevant μ-O and μ-NN contributions, taking into account the orthogonality situation and the molecular symmetry. Figure 6 represents a spin-exchange model that subdivides the grid into the magnetic-exchange components that will be the principal contributors. As the four corner sites can effectively be isolated magnetically, and as the connections 2–13, 3–14, 5–14, 6–15, 8–15, 9–16, 11–16, and 12–13 are orthogonal (see above), the exchange can be modeled as the sum of four dinuclear terms and one tetranuclear term, as defined by the exchange Hamiltonian [Eq. (1)]. J_1 refers to connections with

$$H_{ex} = -J_1\{S_2 \cdot S_3 + S_8 \cdot S_9\} - J_2\{S_5 \cdot S_6 + S_{11} \cdot S_{12}\} - [J_1\{S_{13} \cdot S_{16} + S_{14} \cdot S_{15}\} + J_2\{S_{13} \cdot S_{14} + S_{15} \cdot S_{16}\}] \quad (1)$$

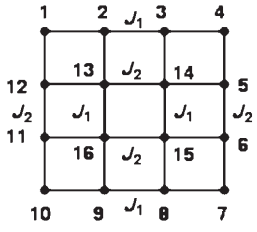

Figure 6. Proposed magnetic exchange model for **1**.

orthogonal oxygen bridges, and J_2 refers to those with nonorthogonal oxygen bridges. The simplifying assumption is also made that exchange through O5 and O8 is the same, because the Cu-O-Cu angles are comparable (123.8° and 121.0°, respectively).

Appropriate exchange equations were written for the dinuclear and tetranuclear components, and these were factored and combined to include corrections for TIP (temperature-independent paramagnetism) and the four "isolated" corner copper(II) sites. In view of the complexity of the exchange model, a remarkably good fit was obtained (solid lines in Figure 5) for $g = 2.21$, $J_1 = -45\ cm^{-1}$, $J_2 = -350\ cm^{-1}$, $TIP = 800 \times 10^{-6}\ cm^3 mol^{-1}$, $10^2 R = 2.3$; ($R = [\Sigma(\chi_{obsd} - \chi_{calcd})^2/\Sigma\chi_{obsd}^2]^{1/2}$). J_1 is associated only with the pyridazine bridges, whereas J_2 is associated with the pyridazine/nonorthogonal oxygen bridging connections. As would be expected, $|J_2|$ is much larger than $|J_1|$, and it is satisfying to compare these values with those associated with comparable simple dinuclear copper compounds involving pyridazine and pyridazine/OH bridges. Weak coupling ($-J = 65\ cm^{-1}$) was found for the compound $[Cu_2(PPD)Cl_4]$, which involves only a magnetically active pyridazine bridge in a similar bonding situation.[18] For compounds with magnetically active combinations of pyridazine and μ-OH, and large Cu-OH-Cu angles (116–126°), $-J$ values in the range 375–450 cm^{-1} were found.[15,16] This comparison strongly supports the assignment of the bridging connectivity in **1** and the prediction of magnetic properties on the basis of the orbital connectivity.

In summary, ligand design and synthesis has led to a viable approach to the specific self-assembly of a supramolecular polymetallic square-grid-shaped Cu_{16} aggregate. The formation of a complete [4 × 4] grid in this case, compared with an incomplete Cu_{12} grid with the closely related ligand L1,[9] is reasonably associated with the addition of sufficient base to fully deprotonate the ligand hydrazone oxygen atoms. This arrangement leads to a complex network of spin-exchange pathways through pyridazine, hydrazone, and exogenous oxygen bridges throughout the grid, which in some cases are effectively switched off because of the preferred orthogonal magnetic connections between copper ions in certain grid positions. This behavior is typical of copper(II) in simpler [2 × 2] and [3 × 3] grids, in which ferromagnetic exchange dominates because of a prevalence of orthogonal connections. However, in the present case, a specific mixture of orthogonal and nonorthogonal connections allows the antiferromagnetic exchange terms to dominate. Fitting of the variable-temperature magnetic data to an appropriate model based on this connectivity gives exchange coupling through μ-pyridazine and μ-pyridazine/O combinations comparable to those of simpler related dinuclear complexes.

Experimental Section

L3: Methyl pyrimidine-2-carboximidate was generated in situ by reaction of 2-cyanopyrimidine (0.73 g, 6.96 mmol) with a solution of sodium methoxide, produced by dissolving sodium metal (0.10 g, 4.35 mmol) in methanol (100 mL). Pyridazine-3,6-dicarbohydrazide (0.68 g, 3.45 mmol; prepared from the reaction of dimethyl pyridazine-3,6-dicarboxylate[16,17] with hydrazine hydrate in methanol) was added to the above solution and the pH was adjusted to 7 with acetic acid. The mixture was refluxed for 18 h. The resulting yellow slurry was filtered and washed with diethyl ether (3 × 15 mL) to yield a yellow powder, which was used without further purification. Yield (1.24 g, 88 %), m.p. > 330 °C. Mass spectrum (major mass peaks, *m/z*): 391.4 ($M-NH_2$), 302.1, 284.1, 149.1. IR (nujol): $\tilde{\nu} = 3309, 3197$ (νNH); 1646 (νC=O); 1600 cm^{-1} (νC=N). Elemental analysis calcd (%) for $C_{16}H_{14}N_{12}O_2 \cdot 0.5\,H_2O$: C 46.27, H 3.64, N 40.47; found: C 46.44, H 3.41, N 40.72.

Compound **1** was synthesized from the reaction of $Cu(CF_3SO_3)_2$ (0.608 mmol) in 1:1 MeOH/CH_3CN (15 mL) with L3 (0.295 mmol). This reaction produced a clear, dark green solution to which aqueous NaOH (4 mL; 0.65 M) was added to achieve a neutral pH. The resulting dark brown solution was stirred with gentle heating for 24 h and then filtered. The filtrate was preserved for crystallization. Brown needle-like crystals, suitable for X-ray diffraction, formed upon standing after 12 days (35 % yield). Elemental analysis calcd (%) for $[(C_{16}H_{12}N_{12}O_2)_6(C_{16}H_{11}N_{12}O_2)_2Cu_{16}(O)_2(OH)_4(H_2O)_2](CF_3SO_3)_6$-$(H_2O)_{66}(CH_3OH)_{10}$: C 25.47, H 4.07, N 19.81; found: C 25.24, H 2.13, N 19.82.

Crystal data for **1**: Orthorhombic, *Pmmn* (no. 59), $a = 25.797(2)$, $b = 29.199(2)$, $c = 16.5920(13)$ Å, $V = 12497.5(18)$ Å^3, $Z = 2$, $\rho_{calcd} = 1.505\ g\,cm^{-3}$, $\mu = 1.482\ mm^{-1}$, final $R_1 = 0.0639$ for $I > 2\sigma(I)$, $wR_2 = 0.1825$ for all data. The intensity data were recorded on a Rigaku AFC8-Saturn 70 system with $Mo_{K\alpha}$ radiation ($\lambda = 0.71070$ Å) at 113(2) K. The structure was solved by direct methods and refined by full-matrix least-squares analysis on F^2 by using SHELXL. NH_2 protons (H4, 5, 10, 11, 16, 17, 22, and 23) were located in difference map positions. However, H23 appeared much lower in the peak list relative to the others, and its occupancy was consequently set to 0.5. The Platon Squeeze[18] procedure was applied to recover 427.1 electrons per unit cell in two voids (total volume 4161.7 Å^3). Disordered solvent water and acetonitrile molecules appeared to be present prior to the application of Squeeze, though a good point atom model could not be achieved for them. The application of Squeeze greatly improved the data statistics and allowed a full anisotropic refinement of the framework structure and counterions. CCDC 644634 contains the supplementary crystallographic data for this paper. These can be obtained free of charge from the Cambridge Crystallographic Data Centre via www.ccdc.cam.ac.uk/data_request/cif.

Variable-temperature magnetic measurements were performed on a Quantum Design MPMS5S magnetometer in DC mode (0.1-T field) with appropriate corrections for the sample holder and diamagnetic complex components.

Received: April 25, 2007
Published online: August 14, 2007

Keywords: copper · grid complexes · magnetic properties · N,O ligands · self-assembly

[1] C. J. Matthews, K. Avery, Z. Xu, L. K. Thompson, L. Zhao, D. O. Miller, K. Biradha, K. Poirier, M. J. Zaworotko, C. Wilson, A. E. Goeta, J. A. K. Howard, *Inorg. Chem.* **1999**, *38*, 5266 – 5276.
[2] L. K. Thompson, L. Zhao, Z. Xu, D. O. Miller, W. M. Reiff, *Inorg. Chem.* **2003**, *42*, 128 – 139.
[3] V. A. Milway, S. M. T. Abedin, V. Niel, T. L. Kelly, L. N. Dawe, S. K. Dey, D. W. Thompson, D. O. Miller, M. S. Alam, P. Müller, L. K. Thompson, *Dalton Trans.* **2006**, 2835 – 2851.
[4] O. Waldmann, R. Koch, S. Schrom, P. Müller, L. Zhao, L. K. Thompson, *Chem. Phys. Lett.* **2000**, *332*, 73 – 78.
[5] O. Waldmann, L. Zhao, L. K. Thompson, *Phys. Rev. Lett.* **2002**, *88*, 066401.

[6] L. K. Thompson, O. Waldmann, Z. Xu, *Coord. Chem. Rev.* **2005**, *249*, 2677 – 2690.
[7] O. Waldmann, H. U. Güdel, T. L. Kelly, L. K. Thompson, *Inorg. Chem.* **2006**, *45*, 3295 – 3300.
[8] L. K. Thompson, C. J. Matthews, L. Zhao, C. Wilson, M. A. Leech, J. A. K. Howard, *J. Chem. Soc. Dalton Trans.* **2001**, 2258 – 2262.
[9] C. J. Matthews, S. T. Onions, G. Morata, M. Bosch Salvia, M. R. J. Elsegood, D. J. Price, *Chem. Commun.* **2003**, 320 – 321.
[10] P. N. W. Baxter, J.-M. Lehn, J. Fischer, M.-T. Youinou, *Angew. Chem.* **1994**, *106*, 2432 – 2434; *Angew. Chem. Int. Ed. Engl.* **1994**, *33*, 2284 – 2287.
[11] P. N. W. Baxter, J.-M. Lehn, G. Baum, D. Fenske, *Chem. Eur. J.* **2000**, *6*, 4510 – 4517.
[12] M. Ruben, J. Rojo, F. J. Romero-Salguero, L. H. Uppadine, J.-M. Lehn, *Angew. Chem.* **2004**, *116*, 3728 – 3747; *Angew. Chem. Int. Ed.* **2004**, *43*, 3644 – 3662.
[13] S. K. Dey, L. K. Thompson, L. N. Dawe, *Chem. Commun.* **2006**, 4967 – 4969.
[14] S. K. Dey, T. S. M. Abedin, L. N. Dawe, S. S. Tandon, J. L. Collins, L. K. Thompson, A. V. Postnikov, M. S. Alam, P. Müller. *Inorg. Chem.*, in press.
[15] L. K. Thompson, T. C. Woon, D. B. Murphy, E. J. Gabe, F. L. Lee, Y. Le Page, *Inorg. Chem.* **1985**, *24*, 4719 – 4725.
[16] L. K. Thompson, S. K. Mandal, E. J. Gabe, F. L. Lee, *Inorg. Chem.* **1987**, *26*, 657 – 664.
[17] L. N. Dawe, T. S. M. Abedin, T. L. Kelly, L. K. Thompson, D. O. Miller, L. Zhao, C. Wilson, M. A. Leech, J. A. K. Howard, *J. Mater. Chem.* **2006**, *16*, 2645 – 2659.
[18] S. K. Mandal, L. K. Thompson, E. J. Gabe, F. L. Lee, *Inorg. Chem.* **1987**, *26*, 2384 – 2389.
[19] G. H. Spencer, Jr., P. C. Cross, K. B. Wiberg, *J. Chem. Phys.* **1961**, *35*, 1939 – 1945.
[20] S. Sueur, M. Lagrenee, F. Abraham, C. Bremard, *J. Heterocycl. Chem.* **1987**, *24*, 1285 – 1289.
[21] A. L. Spek, *J. Appl. Crystallogr.* **2003**, *36*, 7 – 13.

